

We are IntechOpen, the world's leading publisher of Open Access books Built by scientists, for scientists

6,900

Open access books available

186,000

International authors and editors

200M

Downloads

Our authors are among the

154

Countries delivered to

TOP 1%

most cited scientists

12.2%

Contributors from top 500 universities



WEB OF SCIENCE™

Selection of our books indexed in the Book Citation Index
in Web of Science™ Core Collection (BKCI)

Interested in publishing with us?
Contact book.department@intechopen.com

Numbers displayed above are based on latest data collected.
For more information visit www.intechopen.com



Wireless fading channel models: from classical to stochastic differential equations

Mohammed Olama¹, Seddik Djouadi² and Charalambos Charalambous³

¹*Oak Ridge National Laboratory*

²*University of Tennessee*

³*University of Cyprus*

^{1,2}USA, ³Cyprus

1. Introduction

The wireless communications channel constitutes the basic physical link between the transmitter and the receiver antennas. Its modeling has been and continues to be a tantalizing issue, while being one of the most fundamental components based on which transmitters and receivers are designed and optimized. The ultimate performance limits of any communication system are determined by the channel it operates in [1]. Realistic channel models are thus of utmost importance for system design and testing.

In addition to exponential power path-loss, wireless channels suffer from stochastic short term fading (STF) due to multipath, and stochastic long term fading (LTF) due to shadowing depending on the geographical area. STF corresponds to severe signal envelope fluctuations, and occurs in densely built-up areas filled with lots of objects like buildings, vehicles, etc. On the other hand, LTF corresponds to less severe mean signal envelope fluctuations, and occurs in sparsely populated or suburban areas [2-4]. In general, LTF and STF are considered as superimposed and may be treated separately [4].

Ossanna [5] was the pioneer to characterize the statistical properties of the signal received by a mobile user, in terms of interference of incident and reflected waves. His model was better suited for describing fading occurring mainly in suburban areas (LTF environments). It is described by the average power loss due to distance and power loss due to reflection of signals from surfaces, which when measured in dB's give rise to normal distributions, and this implies that the channel attenuation coefficient is log-normally distributed [4]. Furthermore, in mobile communications, the LTF channel models are also characterized by their special correlation characteristics which have been reported in [6-8].

Clarke [9] introduced the first comprehensive scattering model describing STF occurring mainly in urban areas. An easy way to simulate Clarke's model using a computer simulation is described in [10]. This model was later expanded to three-dimensions (3D) by Aulin [11]. An indoor STF was first introduced in [12]. Most of these STF models provide information on the frequency response of the channel, described by the Doppler power spectral density

(DPSD). Aulin [11] presented a methodology to find the Doppler power spectrum by computing the Fourier transform of the autocorrelation function of the channel impulse response with respect to time. A different approach, leading to the same Doppler power spectrum relation was presented by Gans [13]. These STF models suggest various distributions for the received signal amplitude such as Rayleigh, Rician, or Nakagami.

Models based on autoregressive and moving averages (AR) are proposed in [14, 15]. However, these models assume that the channel state is completely observable, which in reality is not the case due to additive noise, and requires long observation intervals. First order Markov models for Raleigh fading have been proposed in [16, 17], and the usefulness of a finite-state Markov channel model is argued in [18].

Mobile-to-mobile (or ad hoc) wireless networks comprise nodes that freely and dynamically self-organize into arbitrary and/or temporary network topology without any fixed infrastructure support [19]. They require direct communication between a mobile transmitter and a mobile receiver over a wireless medium. Such mobile-to-mobile communication systems differ from the conventional cellular systems, where one terminal, the base station, is stationary, and only the mobile station is moving. As a consequence, the statistical properties of mobile-to-mobile links are different from cellular ones [20, 21].

Copious ad hoc networking research exists on layers in the open system interconnection (OSI) model above the physical layer. However, neglecting the physical layer while modeling wireless environment is error prone and should be considered more carefully [22]. The experimental results in [23] show that the factors at the physical layer not only affect the absolute performance of a protocol, but because their impact on different protocols is non-uniform, it can even change the relative ranking among protocols for the same scenario. The importance of the physical layer is demonstrated in [24] by evaluating the Medium Access Control (MAC) performance.

Most of the research conducted on wireless channel modeling, such as [1-4, 25, 26], deals mainly with deterministic wireless channel models. In these models, the speeds of the nodes are assumed to be constant and the statistical characteristics of the received signal are assumed to be fixed with time. But in reality, the propagation environment varies continuously due to mobility of the nodes at variable speeds and movement of objects or scatter across transmitters and receivers resulting in appearance or disappearance of existing paths from one instant to the next. As a result, the current models that assume fixed statistics are unable to capture and track complex time variations in the propagation environment. These time variations compel us to introduce more advanced dynamical models based on stochastic differential equations (SDEs), in order to capture higher order dynamics of the wireless channels. The random variables characterizing the instantaneous power in static (deterministic) channel models are generalized to dynamical (stochastic) models including random processes with time-varying statistics [27-31]. The advantage of using SDE methods is due to computational simplicity simply because estimation and identification can be performed recursively and in real time. Parts of the results appearing in this chapter were presented in [27-31].

This chapter is organized as follows. In Section 2, the general time-varying (TV) wireless channel impulse response is introduced. The TV stochastic LTF, STF, and ad hoc wireless channel models are discussed in Sections 3, 4, and 5, respectively. Link performance for cellular and ad hoc channels is presented in Section 6. Finally, Section 7 provides the conclusion.

2. The General Time-Varying Wireless Channel Impulse Response

The impulse response (IR) of a wireless channel is typically characterized by time variations and time spreading [2]. Time variations are due to the relative motion between the transmitter and the receiver and temporal variations of the propagation environment. Time spreading is due to the fact that the emitted electromagnetic wave arrives at the receiver having undergone reflections, diffraction and scattering from various objects along the way, at different delay times. At the receiver, a random number of signal components, copies of a single emitted signal, arrive via different paths thus having undergone different attenuation, phase shifts and time delays, all of which are random and time-varying. This random number of signal components add vectorially giving rise to signal fluctuations, called multipath fading, which are responsible for the degradation of communication system performance.

The general time-varying (TV) model of a wireless fading channel is typically represented by the following multipath *low-pass* equivalent IR [2]

$$C_l(t; \tau) = \sum_{n=1}^{N(t)} r_n(t, \tau) e^{j\Phi_n(t, \tau)} \delta(\tau - \tau_n(t)) = \sum_{n=1}^{N(t)} (I_n(t, \tau) + jQ_n(t, \tau)) \delta(\tau - \tau_n(t)) \quad (1)$$

where $C_l(t; \tau)$ is the response of the channel at time t , due to an impulse applied at time $t - \tau$, $N(t)$ is the random number of multipath components impinging on the receiver, and the set $\{r_n(t, \tau), \Phi_n(t, \tau), \tau_n(t)\}_{n=1}^{N(t)}$ describes the random TV attenuation, overall phase shift, and arrival time of the different paths, respectively. $\{I_n(t, \tau), Q_n(t, \tau)\}_{n=1}^{N(t)} \triangleq \{r_n(t, \tau) \cos \Phi_n(t, \tau), r_n(t, \tau) \sin \Phi_n(t, \tau)\}_{n=1}^{N(t)}$ are defined as the inphase and quadrature components of each path. Let $s_l(t)$ be the low-pass equivalent representation of the transmitted signal, then the *low-pass* equivalent representation of the received signal is given by

$$y_l(t) = \int_{-\infty}^{\infty} C_l(t; \tau) s_l(t - \tau) d\tau = \sum_{n=1}^{N(t)} r_n(t, \tau_n(t)) e^{j\Phi_n(t, \tau_n(t))} s_l(t - \tau_n(t)) \quad (2)$$

The multipath TV *band-pass* IR is given by [2]

$$C(t; \tau) = \text{Re} \left\{ \sum_{n=1}^{N(t)} \left[r_n(t, \tau) e^{j\Phi_n(t, \tau)} \right] e^{j\omega_c \tau} \delta(\tau - \tau_n(t)) \right\} = \sum_{n=1}^{N(t)} (I_n(t, \tau) \cos \omega_c \tau - Q_n(t, \tau) \sin \omega_c \tau) \delta(\tau - \tau_n(t)) \quad (3)$$

where ω_c is the carrier frequency, and the *band-pass* representation of the received signal is given by

$$y(t) = \sum_{n=1}^{N(t)} \left(I_n(t, \tau_n(t)) \cos \omega_c t - Q_n(t, \tau_n(t)) \sin \omega_c t \right) s_l(t - \tau_n(t)) \quad (4)$$

TV LTF, STF, and ad hoc dynamical channel models are considered in this chapter. The stochastic TV LTF channel modeling is discussed first in the next section.

3. Stochastic LTF Channel Modeling

3.1 The Traditional (Static) LTF Channel Model

In this section, we discuss the existing static models and introduce a general approach on how to derive dynamical models. Before introducing the dynamical LTF channel model that captures both space and time variations, we first summarize and interpret the traditional lognormal shadowing model, which serves as a basis in the development of the subsequent TV model. The traditional (time-invariant) power loss (PL) in dB for a given path is given by [4]

$$PL(d)[\text{dB}] := \overline{PL}(d_0)[\text{dB}] + 10\alpha \log\left(\frac{d}{d_0}\right) + \tilde{Z}, \quad d \geq d_0 \quad (5)$$

where $\overline{PL}(d_0)$ is the average PL in dB at a reference distance d_0 from the transmitter, the distance d corresponds to the transmitter-receiver separation distance, α is the path-loss exponent which depends on the propagating medium, and $\tilde{Z} \sim \mathcal{N}(0; \sigma^2)$ is a zero-mean Gaussian distributed random variable, which represents the variability of PL due to numerous reflections and possibly any other uncertainty of the propagating environment from one observation instant to the next. The average value of the PL described in (5) is

$$\overline{PL}(d)[\text{dB}] := \overline{PL}(d_0)[\text{dB}] + 10\alpha \log\left(\frac{d}{d_0}\right), \quad d \geq d_0 \quad (6)$$

The signal attenuation coefficient, denoted $r(d)$, represents how much the received signal magnitude is attenuated at a distance d with respect to the magnitude of the transmitted signal. It can be represented in terms of the power path loss as [4]

$$r(d) := e^{k \cdot PL(d)[\text{dB}]} \quad \text{where} \quad k = -\ln(10) / 20 \quad (7)$$

Since $PL(d)[\text{dB}]$ is normally distributed, it is clear that the attenuation coefficient, $r(d)$, is log-normally distributed. It can be noticed from (5)-(7) that the statistics of the PL and attenuation coefficient do not depend on time, and therefore these models treat PL as static (time-invariant). They do not take into consideration the relative motion between the transmitter and the receiver, or variations of the propagating environment due to mobility.

Such spatial and time variations of the propagating environment are captured herein by modeling the PL and the envelope of the received signal as random processes that are functions of space and time. Moreover, and perhaps more importantly, traditional models do not take into consideration the correlation properties of the PL in space and at different observation times. In reality, such correlation properties exist, and one way to model them is through stochastic processes, which obey specific type of SDEs.

3.2 Stochastic LTF Channel Models

In transforming the static model to a dynamical model, the random PL in (5) is relaxed to become a random process, denoted by $\{X(t, \tau)\}_{t \geq 0, \tau \geq \tau_0}$, which is a function of both time t and space represented by the time-delay τ , where $\tau = d/c$, d is the path length, c is the speed of light, $\tau_0 = d_0/c$ and d_0 is the reference distance. The signal attenuation is defined by $S(t, \tau) \triangleq e^{kX(t, \tau)}$, where $k = -\ln(10)/20$ [4]. For simplicity, we first introduce the TV lognormal model for a fixed transmitter-receiver separation distance d (or τ) that captures the temporal variations of the propagating environment. Next, we generalize it by allowing both t and τ to vary as the transmitter and receiver, as well as scatters, are allowed to move at variable speeds. This induces spatio-temporal variations in the propagating environment.

When τ is fixed, the proposed model captures the dependence of $\{X(t, \tau)\}_{t \geq 0, \tau \geq \tau_0}$ on time t . This corresponds to examining the time variations of the propagating environment for fixed transmitter-receiver separation distance. The process $\{X(t, \tau)\}_{t \geq 0, \tau \geq \tau_0}$ represents how much power the signal loses at a particular location as a function of time. However, since for a fixed distance d , the PL should be a function of distance, we choose to generate $\{X(t, \tau)\}_{t \geq 0, \tau \geq \tau_0}$ by a mean-reverting version of a general linear SDE given by [29, 30]

$$\begin{aligned} dX(t, \tau) &= \beta(t, \tau)(\gamma(t, \tau) - X(t, \tau))dt + \delta(t, \tau)dW(t), \\ X(t_0, \tau) &\sim N(\overline{PL}(d)[dB]; \sigma^2) \end{aligned} \quad (8)$$

where $\{W(t)\}_{t \geq 0}$ is the standard Brownian motion (zero drift, unit variance) which is assumed to be independent of $X(t_0, \tau)$, $N(\mu; \kappa)$ denotes a Gaussian random variable with mean μ and variance κ , and $\overline{PL}(d)[dB]$ is the average path-loss in dB. The parameter $\gamma(t, \tau)$ models the average time-varying PL at distance d from the transmitter, which corresponds to $\overline{PL}(d)[dB]$ at d indexed by t . This model tracks and converges to $\gamma(t, \tau)$ as time progresses. The instantaneous drift $\beta(t, \tau)(\gamma(t, \tau) - X(t, \tau))$ represents the effect of pulling the process towards $\gamma(t, \tau)$, while $\beta(t, \tau)$ represents the speed of adjustment towards the mean. Finally, $\delta(t, \tau)$ controls the instantaneous variance or volatility of the process for the instantaneous drift.

Let $\{\theta(t, \tau)\}_{t \geq 0} \triangleq \{\beta(t, \tau), \gamma(t, \tau), \delta(t, \tau)\}_{t \geq 0}$. If the random processes in $\{\theta(t, \tau)\}_{t \geq 0}$ are measurable and bounded [32], then (8) has a unique solution for every $X(t_0, \tau)$ given by [30]

$$X(t, \tau) = e^{-\beta([t, t_0], \tau)} \left(X(t_0, \tau) + \int_{t_0}^t e^{\beta([u, t_0], \tau)} (\beta(u, \tau) \gamma(u, \tau) du + \delta(u, \tau) dW(u)) \right) \quad (9)$$

where $\beta([t, t_0], \tau) \triangleq \int_{t_0}^t \beta(u, \tau) du$. Moreover, using Ito's stochastic differential rule [32] on

$S(t, \tau) = e^{kX(t, \tau)}$ the attenuation coefficient obeys the following SDE

$$dS(t, \tau) = S(t, \tau) \left[\left(k\beta(t, \tau)[\gamma(t, \tau) - \frac{1}{k} \ln S(t, \tau)] + \frac{1}{2} k^2 \delta^2(t, \tau) \right) dt + k\delta(t, \tau) dW(t) \right] \quad (10)$$

$$S(t_0, \tau) = e^{kX(t_0, \tau)}$$

This model captures the temporal variations of the propagating environment as the random parameters $\{\theta(t, \tau)\}_{t \geq 0}$ can be used to model the TV characteristics of the channel for the particular location τ . A different location is characterized by a different set of parameters $\{\theta(t, \tau)\}$.

Now, let us consider the special case when the parameters $\theta(t, \tau)$ are time invariant, i.e., $\theta(\tau) \triangleq \{\beta(\tau), \gamma(\tau), \delta(\tau)\}$. In this case we need to show that the expected value of the dynamic PL $X(t, \tau)$, denoted by $E[X(t, \tau)]$, converges to the traditional average PL in (6). The solution of the SDE model in (8) for the time-invariant case satisfies

$$X(t, \tau) = e^{-\beta(\tau)(t-t_0)} X(t_0, \tau) + \gamma(\tau) \left(1 - e^{-\beta(\tau)(t-t_0)} \right) + \delta(\tau) \int_{t_0}^t e^{-\beta(\tau)(t-u)} dW(u) \quad (11)$$

where for a given set of time-invariant parameters $\theta(\tau)$ and if the initial $X(t_0, \tau)$ is Gaussian or fixed, then the distribution of $X(t, \tau)$ is Gaussian with mean and variance given by [32]

$$E[X(t, \tau)] = \gamma(\tau) \left(1 - e^{-\beta(\tau)(t-t_0)} \right) + e^{-\beta(\tau)(t-t_0)} E\{X(t_0, \tau)\}$$

$$\text{Var}[X(t, \tau)] = \delta^2(\tau) \left(\frac{1 - e^{-2\beta(\tau)(t-t_0)}}{2\beta(\tau)} \right) + e^{-2\beta(\tau)(t-t_0)} \text{Var}(X(t_0, \tau)) \quad (12)$$

Expression (12) of the mean and variance shows that the statistics of the communication channel model vary as a function of both time t and space τ . As the observation instant, t , becomes large, the random process $\{X(t, \tau)\}$ converges to a Gaussian random variable with mean $\gamma(\tau) = \overline{PL}(d)$ [dB] and variance $\delta^2(\tau) / 2\beta(\tau)$. Therefore, the traditional lognormal model in (5) is a special case of the general TV LTF model in (8). Moreover, the distribution of $S(t, \tau) = e^{kX(t, \tau)}$ is lognormal with mean and variance

$$E[S(t, \tau)] = \exp\left(\frac{2kE[X(t, \tau)] + k^2\text{Var}[X(t, \tau)]}{2}\right) \quad (13)$$

$$\text{Var}[S(t, \tau)] = \exp\left(2kE[X(t, \tau)] + 2k^2\text{Var}[X(t, \tau)]\right) - \exp\left(2kE[X(t, \tau)] + k^2\text{Var}[X(t, \tau)]\right)$$

Now, let's go back to the more general case in which $\{\theta(t, \tau)\}_{t \geq 0} \triangleq \{\beta(t, \tau), \gamma(t, \tau), \delta(t, \tau)\}_{t \geq 0}$. At a particular location τ , the mean of the PL process $E[X(t, \tau)]$ is required to track the time variations of the average PL. This is illustrated in the following example.

Example 1 [30]: Let

$$\gamma(t, \tau) = \gamma_m(\tau) \left(1 + 0.15e^{-2t/T} \sin\left(\frac{10\pi t}{T}\right) \right) \quad (14)$$

where $\gamma_m(\tau)$ is the average PL at a specific location τ , T is the observation interval, $\delta(t, \tau) = 1400$ and $\beta(t, \tau) = 225000$ (these parameters are determined from experimental measurements), where for simplicity $\delta(t, \tau)$ and $\beta(t, \tau)$ are chosen to be constant, but in general they are functions of both t and τ . The variations of $X(t, \tau)$ as a function of distance and time are represented in Figure 1. The temporal variations of the environment are captured by a TV $\gamma(t, \tau)$ which fluctuates around different average PLs γ_m 's, so that each curve corresponds to a different location. It is noticed in Figure 1 that as time progresses, the process $X(t, \tau)$ is pulled towards $\gamma(t, \tau)$. The speed of adjustment towards $\gamma(t, \tau)$ can be controlled by choosing different values of $\beta(t, \tau)$.

Next, the general spatio-temporal lognormal model is introduced by generalizing the previous model to capture both space and time variations, using the fact that $\gamma(t, \tau)$ is a function of both t and τ . In this case, besides initial distances, the motion of mobiles, i.e., their velocities and directions of motion with respect to their base stations are important factors to evaluate TV PLs for the links involved. This is illustrated in a simple way for the case of a single transmitter and a single receiver as follows: Consider a base station (receiver) at an initial distance d from a mobile (transmitter) that moves with a certain constant velocity v in a direction defined by an arbitrary constant angle θ , where θ is the angle between the direction of motion of the mobile and the distance vector that starts from

the receiver towards the transmitter as shown in Figure 2. At time t , the distance from the transmitter to the receiver, $d(t)$, is given by

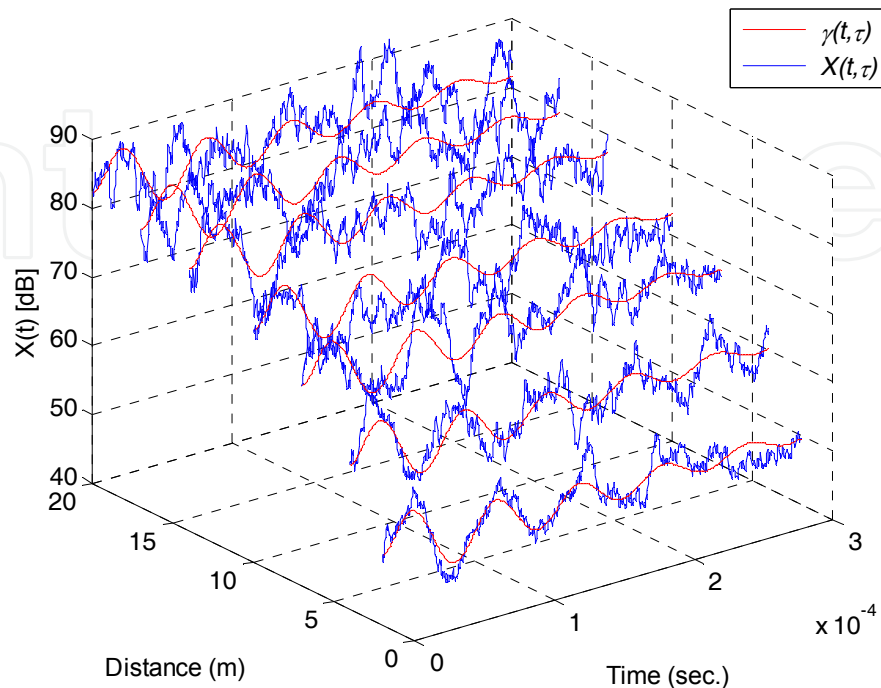


Fig. 1. Mean-reverting power path-loss as a function of t and τ , for the time-varying $\gamma(t, \tau)$ in Example 1.

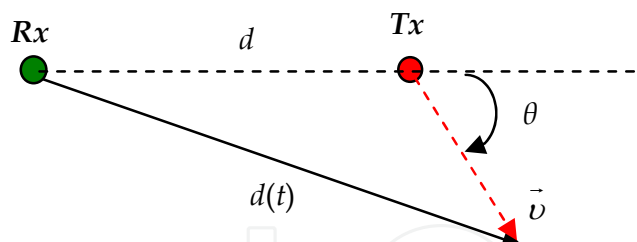


Fig. 2. A transmitter at a distance d from a receiver moves with a velocity v and in the direction given by θ with respect to the transmitter-receiver axis.

$$d(t) = \sqrt{(d + tv \cos \theta)^2 + (tv \sin \theta)^2} = \sqrt{d^2 + (vt)^2 + 2dvt \cos \theta} \quad (15)$$

Therefore, the average PL at that location is given by

$$\gamma(t, \tau) = \overline{PL}(d(t)) [dB] = \overline{PL}(d_0) [dB] + 10\alpha \log \frac{d(t)}{d_0} + \xi(t), \quad d(t) \geq d_0 \quad (16)$$

where $\overline{PL}(d_0)$ is the average PL in dB at a reference distance d_0 , $d(t)$ is defined in (15), α is the path-loss exponent and $\xi(t)$ is an arbitrary function of time representing additional

temporal variations in the propagating environment like the appearance and disappearance of additional scatters.

Now, suppose the mobile moves with an arbitrary velocity, $(v_x(t), v_y(t))$, in the x-y plane, where $v_x(t), v_y(t)$ denote the instantaneous velocity components in the x and y directions, respectively. The instantaneous distance from the receiver is thus described by

$$d(t) = \sqrt{\left(d + \int_0^t v_x(t) dt\right)^2 + \left(\int_0^t v_y(t) dt\right)^2} \quad (17)$$

The parameter $\gamma(t, \tau)$ is used in the TV lognormal model (8) to obtain a general spatio-temporal lognormal channel model. This is illustrated in the following example.

Example 2 [30]: Consider a mobile moving at sinusoidal velocity with average speed 80 Km/hr, initial distance $d=50$ meters, $\theta=135$ degrees, and $\xi(t)=0$. Figure 3 shows the mean reverting PL $X(t, \tau)$, $\gamma(t, \tau)$, $E[X(t, \tau)]$, and the velocity of the mobile $v(t)$ and distance $d(t)$ as a function of time. It can be seen that the mean of $X(t, \tau)$ coincides with the average PL $\gamma(t, \tau)$ and tracks the movement of the mobile. Moreover, the variation of $X(t, \tau)$ is due to uncertainties in the wireless channel such as movements of objects or obstacles between transmitter and receiver that are captured by the spatio-temporal lognormal model (8) and (16). Additional time variations of the propagating environment, while the mobile is moving, can be captured by using the TV PL coefficient $\alpha(t)$ in (16) in addition to the TV parameters $\beta(t, \tau)$ and $\delta(t, \tau)$, or simply by $\xi(t)$. The stochastic STF channel model is discussed in the next section.

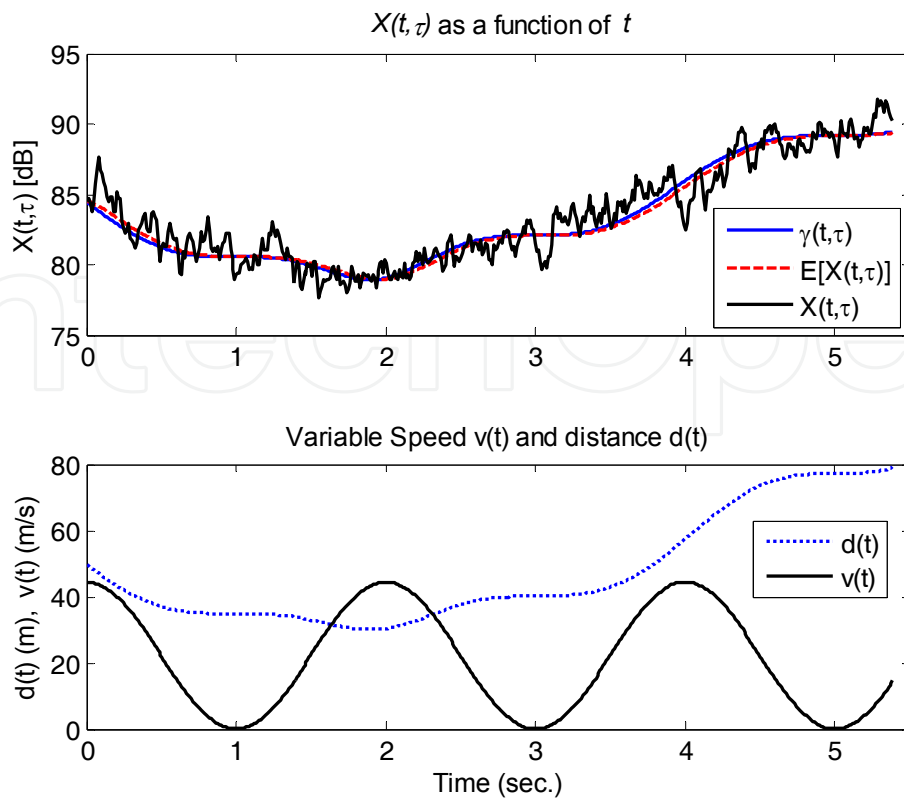


Fig. 3. Mean-reverting power path-loss $X(t, \tau)$ for the TV LTF wireless channel model in Example 2.

4. Stochastic STF Channel Modeling

4.1 The Deterministic DPSD of Wireless Channels

The traditional STF model is based on Ossanna [5] and later Clarke [9] and Aulin's [11] developments. Aulin's model is shown in Figure 4. This model assumes that at each point between a transmitter and a receiver, the total received wave consists of the superposition of N plane waves each having traveled via a different path. The n th wave is characterized by its field vector $E_n(t)$ given by [11]

$$E_n(t) = \text{Re} \left\{ r_n(t) e^{j\Phi_n(t)} e^{j\omega_c t} \right\} = I_n(t) \cos \omega_c t - Q_n(t) \sin \omega_c t \quad (18)$$

where $\{I_n(t), Q_n(t)\}$ are the inphase and quadrature components for the n th wave, respectively, $r_n(t) = \sqrt{I_n^2(t) + Q_n^2(t)}$ is the signal envelope, $\Phi_n(t) = \tan^{-1}(Q_n(t)/I_n(t))$ is the phase, and ω_c is the carrier frequency. The total field $E(t)$ can be written as

$$E(t) = \sum_{n=1}^N E_n(t) = I(t) \cos \omega_c t - Q(t) \sin \omega_c t \quad (19)$$

where $\{I(t), Q(t)\}$ are inphase and quadrature components of the total wave, respectively, with $I(t) = \sum_{n=1}^N I_n(t)$ and $Q(t) = \sum_{n=1}^N Q_n(t)$. An application of the central limit theorem

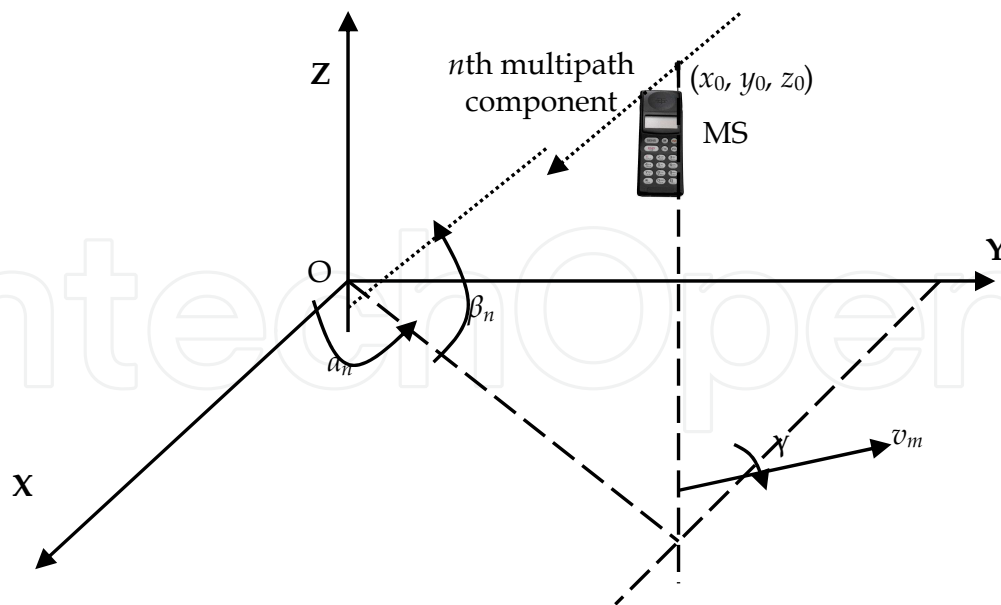


Fig. 4. Aulin's 3D multipath channel model.

states that for large N , the inphase and quadrature components have Gaussian distributions $\mathcal{N}(\bar{x}; \sigma^2)$ [9]. The mean is $\bar{x} = E\{I(t)\} = E\{Q(t)\}$ and the variance is $\sigma^2 = \text{Var}\{I(t)\} = \text{Var}\{Q(t)\}$. In the case where there is non-line-of-sight (NLOS), then the mean $\bar{x} = 0$ and the received signal amplitude has Rayleigh distribution. In the presence of line-of-sight (LOS) component, $\bar{x} \neq 0$ and the received signal is Rician distributed. Also, it is assumed that $I(t)$ and $Q(t)$ are uncorrelated and thus independent since they are Gaussian distributed [11].

Dependent on the mobile speed, wavelength, and angle of incidence, the Doppler frequency shifts on the multipath rays give rise to a DPSD. The DPSD is defined as the Fourier transform of the autocorrelation function of the channel, and represents the amount of power at various frequencies. Define $\{\alpha_n, \beta_n\}$ as the direction of the incident wave onto the receiver as illustrated in Figure 4. For the case when α_n is uniformly distributed and β_n is fixed, the deterministic DPSD, $S(f)$, is given by [25]

$$S(f) = \begin{cases} \frac{E_0}{4\pi} \frac{1/f_m}{\sqrt{1 - \left(\frac{f}{f_m}\right)^2}}, & |f| < f_m \\ 0, & \text{otherwise} \end{cases} \quad (20)$$

where f_m is the maximum Doppler frequency, and $E_0/2 = \text{Var}\{I(t)\} = \text{Var}\{Q(t)\}$. A more complex, but realistic, expression for the DPSD, which assumes β_n has probability density function $p_\beta(\beta) = \frac{\cos \beta}{2 \sin \beta_m}$ where $|\beta| \leq |\beta_m| \leq \frac{\pi}{2}$, and for small angles β_m , is given by [11]

$$S(f) = \begin{cases} 0, & |f| > f_m \\ \frac{E_0}{4f_m \sin \beta_m}, & f_m \cos \beta_m \leq |f| \leq f_m \\ \frac{E_0}{4\pi f_m \sin \beta_m} \left[\frac{\pi}{2} - \sin^{-1} \left(\frac{2 \cos^2 \beta_m - 1 - (f/f_m)^2}{1 - (f/f_m)^2} \right) \right], & |f| < f_m \cos \beta_m \end{cases} \quad (21)$$

Expression (21) is illustrated in Figure 5 for different values of mobile speed. Notice that the direction of motion does not play a role because of the uniform scattering assumption, and that the DPSDs described in (20) and (21) are band limited.

The DPSD is the fundamental channel characteristic on which STF dynamical models are based on. The approach presented here is based on traditional system theory using the state space approach [33] while capturing the spectral characteristics of the channel. The main idea in constructing dynamical models for STF channels is to factorize the deterministic DPSD into an approximate n th order even transfer function, and then use a stochastic realization [32] to obtain a state space representation for the inphase and quadrature components.

The wireless channel is considered as a dynamical system for which the input-output map is described in (1) and (3). In practice, one obtains from measurements the power spectral density of the output, and with the knowledge of the power spectral density of the input the power spectral density of the transfer function (wireless channel) can be deduced as

$$S_{yy}(f) = |H(f)|^2 S_{xx}(f) \quad (22)$$

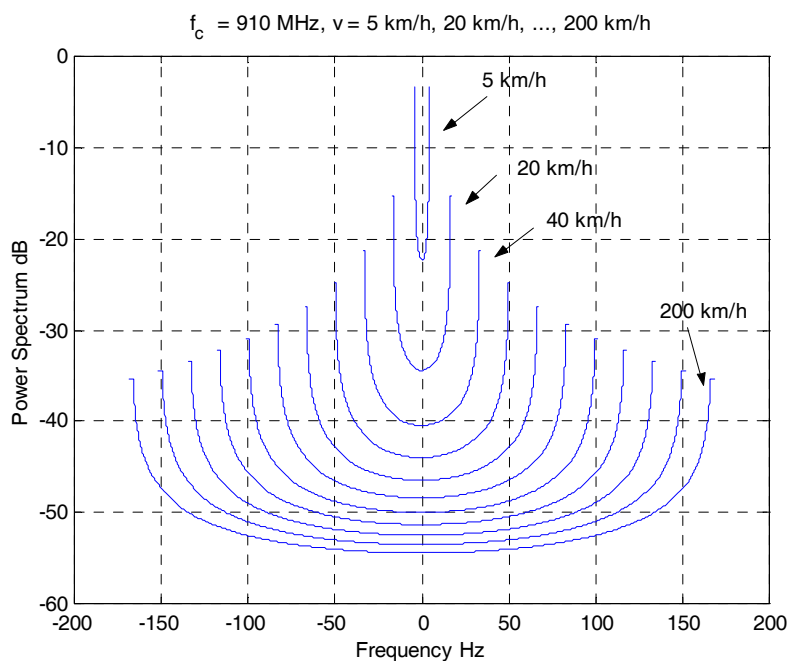


Fig. 5. DPSD for different values of mobile speed ($\beta_m = 10$ degrees).

where $x(t)$ is a random process with power spectral density $S_{xx}(f)$ representing the input signal to the channel, $y(t)$ is a random process with power spectral density $S_{yy}(f)$ representing the output signal of the channel, and $H(f)$ is the frequency response of the channel, which is the Fourier transform of the channel IR.

In general, in order to identify the random process associated with the DPSD, $S(f)$, in (20) or (21) in the form of an SDE, we need to find a transfer function, $H(f)$ whose magnitude square equals $S(f)$, i.e. $S(f)=|H(f)|^2$. This is equivalent to $S(s)=H(s)H(-s)$, where $s=i2\pi f$ and $i=\sqrt{-1}$. That is, we need to factorize the DPSD. This is an old problem which had been studied by Paley and Wiener [34] and is reformulated here as follows:

Given a non-negative integrable function, $S(f)$, such that the Paley-Wiener condition

$$\int_{-\infty}^{\infty} \left[\frac{|\log S(f)|}{(1+f^2)} \right] df < \infty$$

is satisfied, then there exists a causal, stable, minimum-phase

function $H(f)$, such that $|H(f)|^2=S(f)$, implying that $S(f)$ is factorizable, namely, $S(s)=H(s)H(-s)$. It can be seen that the Paley-Wiener condition is not satisfied when $S(f)$ is band limited (and therefore it is not factorizable), which is the case for wireless links. In order to factorize it, the deterministic DPSD has to be first approximated by a *rational* transfer function, denoted $\tilde{S}(f)$, and is discussed next.

4.2 Approximating the Deterministic DPSD

A number of rational approximation methods can be used to approximate the deterministic DPSD [35], the choice of which depends on the complexity and the required accuracy. The order of approximation dictates how close the approximate curve would be to the actual one. Higher order approximations capture higher order dynamics, and provide better approximations for the DPSD, however computations become more involved. In this section, we consider a simple approximating method which uses a 4th order stable, minimum phase, real, rational approximate transfer function. In Section 5.2, we consider the complex cepstrum approximation algorithm [36], which is based on the Gauss-Newton method for iterative search, and is more accurate than the simple approximating method but requires more computations.

In the simple approximating method, a 4th order even transfer function $\tilde{S}(s)$, is used to approximate the deterministic cellular DPSD, $S(s)$. The approximate function $\tilde{S}(s)=H(s)H(-s)$ is given by [28]

$$\tilde{S}(s) = \frac{K^2}{s^4 + 2\omega_n^2(1 - 2\zeta^2)s^2 + \omega_n^4}, \quad H(s) = \frac{K}{s^2 + 2\zeta\omega_n s + \omega_n^2} \quad (23)$$

Equation (23) has three arbitrary parameters $\{\zeta, \omega_n, K\}$, which can be adjusted such that the approximate curve coincides with the actual curve at different points. The reason for presenting 4th order approximation of the DPSD is that we can compute explicit expressions for the constants $\{\zeta, \omega_n, K\}$ as functions of specific points on the data-graphs of the DPSD. In fact, if the approximate density $\tilde{S}(f)$ coincides with the exact density $S(f)$ at $f=0$ and $f=f_{\max}$, then the arbitrary parameters $\{\zeta, \omega_n, K\}$ are computed explicitly as

$$\zeta = \sqrt{\frac{1}{2} \left(1 - \sqrt{1 - \frac{S(0)}{S(f_{\max})}} \right)}, \quad \omega_n = \frac{2\pi f_{\max}}{\sqrt{1 - 2\zeta^2}}, \quad K = \omega_n^2 \sqrt{S(0)} \quad (24)$$

Figure 6 shows $S(f)$ and its approximation $\tilde{S}(f)$ via a 4th order even function. In the next section, the approximated DPSD is used to develop stochastic STF channel models.

4.3 Stochastic STF Channel Models

A stochastic realization is used here to obtain a state space representation for the inphase and quadrature components [32]. The SDE, which corresponds to $H(s)$ in (23) is

$$d^2x(t) + 2\zeta\omega_n dx(t) + \omega_n^2 x(t)dt = KdW(t), \quad \dot{x}(0), x(0) \text{ are given} \quad (25)$$

where $\{dW(t)\}_{t \geq 0}$ is a white-noise process. Equation (25) can be rewritten in terms of inphase and quadrature components as

$$\begin{aligned} d^2x_I(t) + 2\zeta\omega_n dx_I(t) + \omega_n^2 x_I(t)dt &= KdW_I(t), \quad \dot{x}_I(0), x_I(0) \text{ are given} \\ d^2x_Q(t) + 2\zeta\omega_n dx_Q(t) + \omega_n^2 x_Q(t)dt &= KdW_Q(t), \quad \dot{x}_Q(0), x_Q(0) \text{ are given} \end{aligned} \quad (26)$$

where $\{dW_I(t)\}_{t \geq 0}$ and $\{dW_Q(t)\}_{t \geq 0}$ are two independent and identically distributed (i.i.d.) white Gaussian noises.

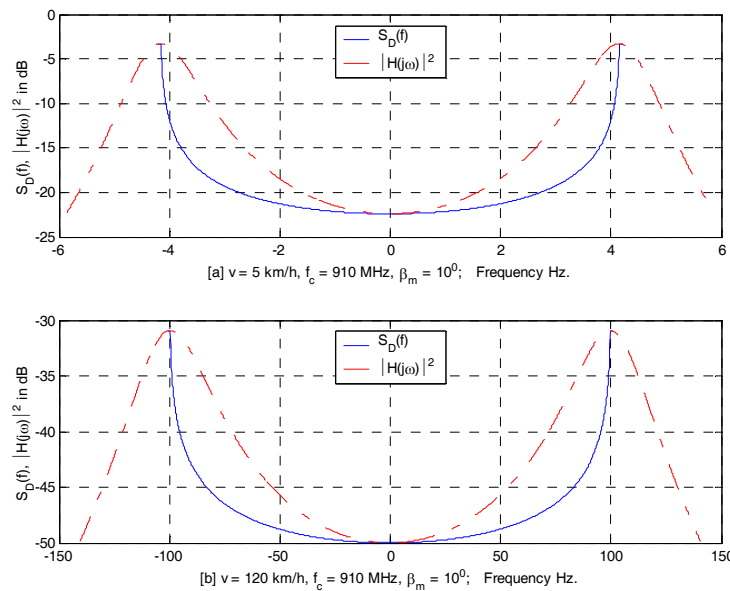


Fig. 6. DPSD, $S_D(f)$, and its approximation $\tilde{S}(\omega) = |H(j\omega)|^2$ via a 4th order transfer function for mobile speed of (a) 5 km/hr and (b) 120 km/hr.

Several stochastic realizations [32] can be used to obtain a state space representation for the inphase and quadrature components of STF channel models. For example, the stochastic observable canonical form (OCF) realization [33] can be used to realize (26) for the inphase and quadrature components for the j th path as

$$\begin{aligned}
 \begin{bmatrix} dX_{I,j}^1(t) \\ dX_{I,j}^2(t) \end{bmatrix} &= \begin{bmatrix} 0 & 1 \\ -\omega_n^2 & -2\xi_n\omega_n \end{bmatrix} \begin{bmatrix} X_{I,j}^1(t) \\ X_{I,j}^2(t) \end{bmatrix} dt + \begin{bmatrix} 0 \\ K \end{bmatrix} dW_j^I(t), \quad \begin{bmatrix} X_{I,j}^1(0) \\ X_{I,j}^2(0) \end{bmatrix}, \\
 I_j(t) &= \begin{bmatrix} 1 & 0 \end{bmatrix} \begin{bmatrix} X_{I,j}^1(t) \\ X_{I,j}^2(t) \end{bmatrix} + f_j^I(t), \\
 \begin{bmatrix} dX_{Q,j}^1(t) \\ dX_{Q,j}^2(t) \end{bmatrix} &= \begin{bmatrix} 0 & 1 \\ -\omega_n^2 & -2\xi_n\omega_n \end{bmatrix} \begin{bmatrix} X_{Q,j}^1(t) \\ X_{Q,j}^2(t) \end{bmatrix} dt + \begin{bmatrix} 0 \\ K \end{bmatrix} dW_j^Q(t), \quad \begin{bmatrix} X_{Q,j}^1(0) \\ X_{Q,j}^2(0) \end{bmatrix}, \\
 Q_j(t) &= \begin{bmatrix} 1 & 0 \end{bmatrix} \begin{bmatrix} X_{Q,j}^1(t) \\ X_{Q,j}^2(t) \end{bmatrix} + f_j^Q(t)
 \end{aligned} \tag{27}$$

where $X_{I,j}(t) = [X_{I,j}^1(t) \ X_{I,j}^2(t)]^T$ and $X_{Q,j}(t) = [X_{Q,j}^1(t) \ X_{Q,j}^2(t)]^T$ are state vectors of the inphase and quadrature components. $I_j(t)$ and $Q_j(t)$ correspond to the inphase and quadrature components, respectively, $\{W_j^I(t)\}_{t \geq 0}$ and $\{W_j^Q(t)\}_{t \geq 0}$ are independent standard Brownian motions, which correspond to the inphase and quadrature components of the j th path respectively, the parameters $\{\xi, \omega_n, K\}$ are obtained from the approximation of the

deterministic DPSD, and $f_j^I(t)$ and $f_j^Q(t)$ are arbitrary functions representing the LOS of the inphase and quadrature components respectively, characterizing further dynamic variations in the environment.

Expression (27) for the j th path can be written in compact form as

$$\begin{aligned} \begin{bmatrix} dX_I(t) \\ dX_Q(t) \end{bmatrix} &= \begin{bmatrix} A_I & 0 \\ 0 & A_Q \end{bmatrix} \begin{bmatrix} X_I(t) \\ X_Q(t) \end{bmatrix} dt + \begin{bmatrix} B_I & 0 \\ 0 & B_Q \end{bmatrix} \begin{bmatrix} dW_I(t) \\ dW_Q(t) \end{bmatrix} \\ \begin{bmatrix} I(t) \\ Q(t) \end{bmatrix} &= \begin{bmatrix} C_I & 0 \\ 0 & C_Q \end{bmatrix} \begin{bmatrix} X_I(t) \\ X_Q(t) \end{bmatrix} + \begin{bmatrix} f_I(t) \\ f_Q(t) \end{bmatrix} \end{aligned} \quad (28)$$

where

$$A_I = A_Q = \begin{bmatrix} 0 & 1 \\ -\omega_n^2 & -2\xi_n\omega_n \end{bmatrix}, \quad B_I = B_Q = \begin{bmatrix} 0 \\ K \end{bmatrix}, \quad C_I = C_Q = [1 \quad 0] \quad (29)$$

$\{W_I(t), W_Q(t)\}_{t \geq 0}$ are independent standard Brownian motions which are independent of the initial random variables $X_I(0)$ and $X_Q(0)$, and $\{f_I(s), f_Q(s); 0 \leq s \leq t\}$ are random processes representing the inphase and quadrature LOS components, respectively. The band-pass representation of the received signal corresponding to the j th path is given as

$$y(t) = \left[(C_I X_I(t) + f_I(t)) \cos \omega_c t - (C_Q X_Q(t) + f_Q(t)) \sin \omega_c t \right] s_j(t - \tau_j) + v(t) \quad (30)$$

where $v(t)$ is the measurement noise. As the DPSD varies from one instant to the next, the channel parameters $\{\zeta, \omega_n, K\}$ also vary in time, and have to be estimated on-line from time domain measurements. Without loss of generality, we consider the case of flat fading, in which the mobile-to-mobile channel has purely multiplicative effect on the signal and the multipath components are not resolvable, and can be considered as a single path [2]. The frequency selective fading case can be handled by including multiple time-delayed echoes. In this case, the delay spread has to be estimated. A sounding device is usually dedicated to estimate the time delay of each discrete path such as Rake receiver [26]. Following the state space representation in (28) and the band pass representation of the received signal in (30), the fading channel can be represented using a general stochastic state space representation of the form [28]

$$\begin{aligned} dX(t) &= A(t)X(t)dt + B(t)dW(t) \\ y(t) &= C(t)X(t) + D(t)v(t) \end{aligned} \quad (31)$$

where

$$\begin{aligned}
 X(t) &= [X_I(t) \quad X_Q(t)]^T, \quad A(t) = \begin{bmatrix} A_I(t) & 0 \\ 0 & A_Q(t) \end{bmatrix}, \quad B(t) = \begin{bmatrix} B_I(t) & 0 \\ 0 & B_Q(t) \end{bmatrix}, \\
 C(t) &= [\cos(\omega_c t)C_I \quad -\sin(\omega_c t)C_Q], \quad D(t) = [\cos(\omega_c t) \quad -\sin(\omega_c t)] \\
 v(t) &= [v_I(t) \quad v_Q(t)]^T, \quad dW(t) = [dW^I(t) \quad dW^Q(t)]^T
 \end{aligned} \tag{32}$$

In this case, $y(t)$ represents the received signal measurements, $X(t)$ is the state variable of the inphase and quadrature components, and $v(t)$ is the measurement noise.

Time domain simulation of STF channels can be performed by passing two independent white noise processes through two identical filters, $\tilde{H}(s)$, obtained from the factorization of the deterministic DPSD, one for the inphase and the other for the quadrature component [4], and realized in their state-space form as described in (28) and (29).

Example 3: Consider a flat fading wireless channel with the following parameters: $f_c = 900$ MHz, $v = 80$ km/h, $\beta_m = 10^\circ$, and $f_j^I(t) = f_j^Q(t) = 0$. Time domain simulation of the inphase and quadrature components, attenuation coefficient, phase angle, input signal, and received signal are shown in Figures 7-9. The inphase and quadrature components have been produced using (28) and (29), while the received signal is reproduced using (30). The simulation of the dynamical STF channel is performed using Simulink in Matlab [37].

4.4 Solution to the Stochastic State Space Model

The stochastic TV state space model described in (31) and (32) has a solution [32, 38]

$$X_L(t) = \Phi_L(t, t_0) \left[X_L(t_0) + \int_{t_0}^t \Phi_L^{-1}(u, t_0) B_L(u) dW_L(u) \right] \tag{33}$$

where $L = I$ or Q , and $\Phi_L(t, t_0)$ is the fundamental matrix, which satisfies $\dot{\Phi}_L(t, t_0) = A_L(t)\Phi_L(t, t_0)$ and $\Phi_L(t_0, t_0)$ is the identity matrix.

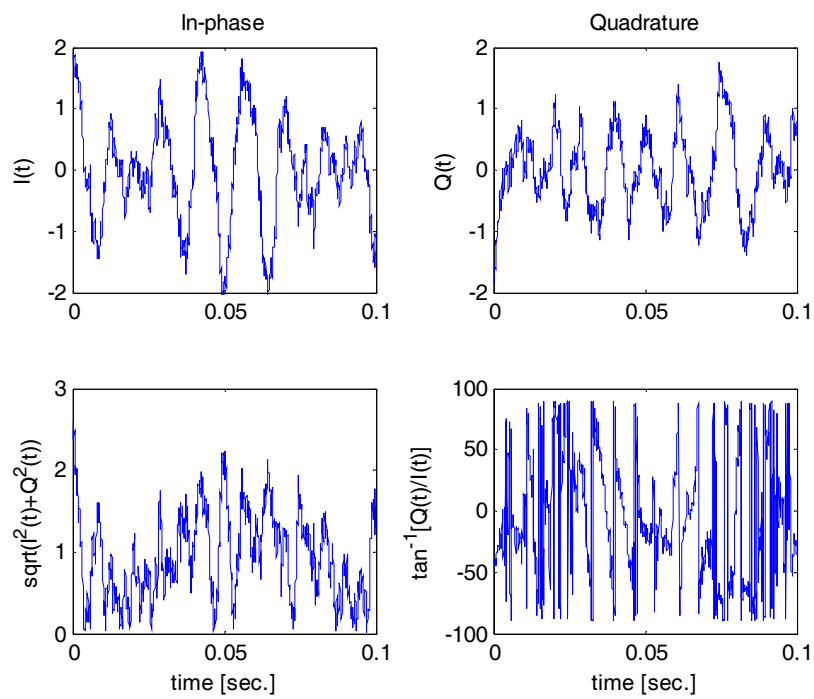


Fig. 7. Inphase and quadrature components, attenuation coefficient, and phase angle of the STF wireless channel in Example 3.

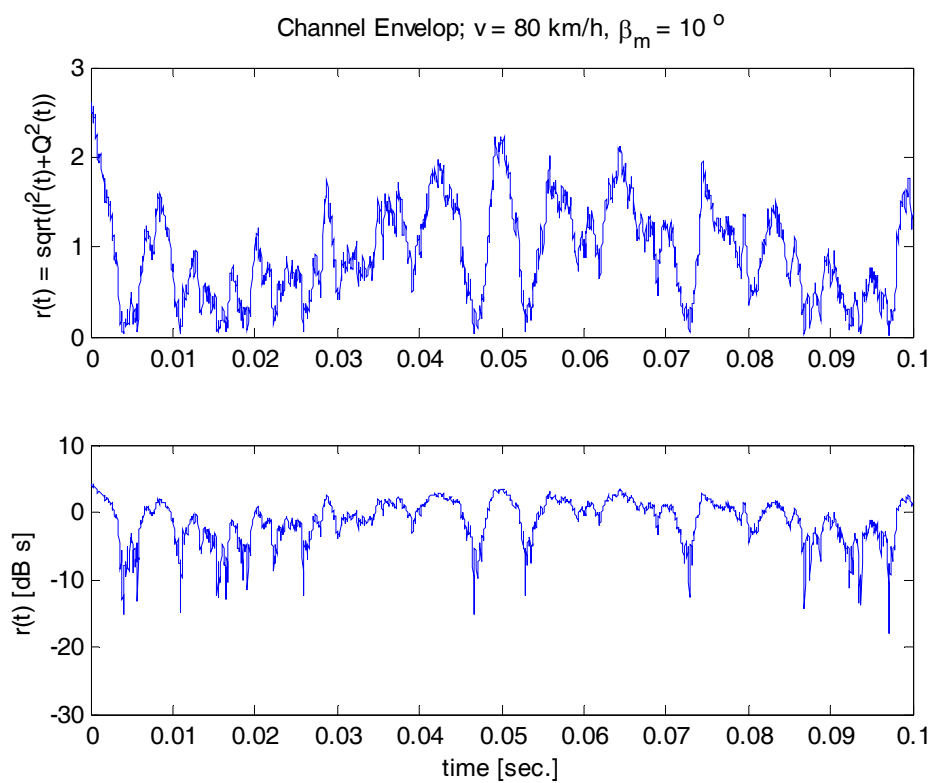


Fig. 8. Attenuation coefficient in absolute units and in dB's for the STF wireless channel in Example 3.

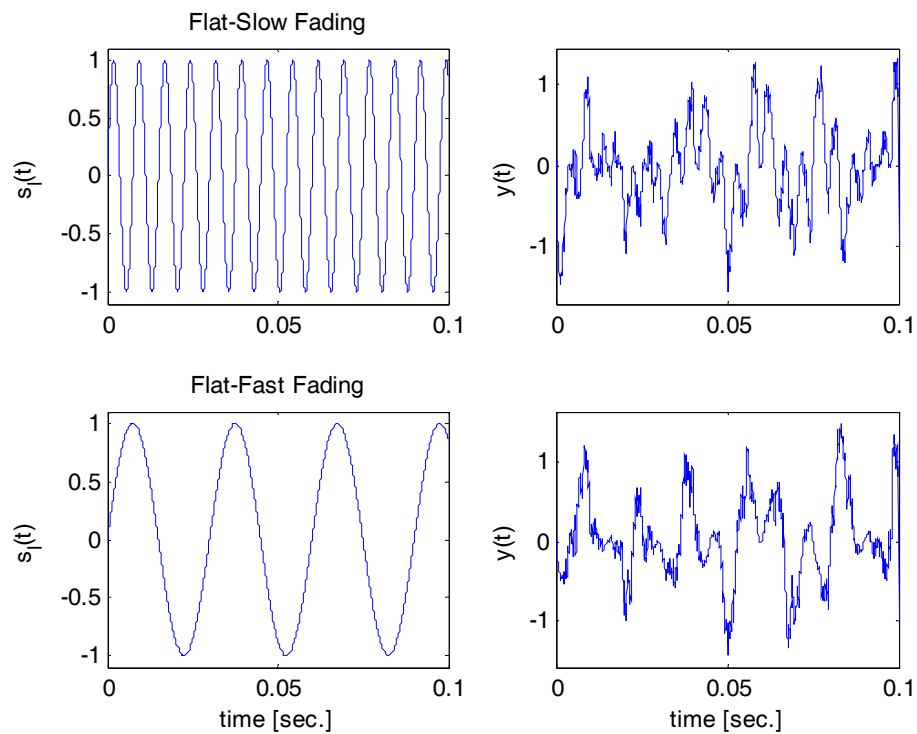


Fig. 9. Input signal, $s_i(t)$, and the corresponding received signal, $y(t)$, for flat slow fading (top) and flat fast fading conditions (bottom).

Further computations show that the mean of $X_L(t)$ is given by [32]

$$E[X_L(t)] = \Phi_L(t, t_0)E[X_L(t_0)] \quad (34)$$

and the covariance matrix of $X_L(t)$ is given by

$$\Sigma_L(t) = \Phi_L(t, t_0) \left[\text{Var}[X_L(t_0)] + \int_{t_0}^t \Phi_L^{-1}(u, t_0) B_L(u) B_L^T(u) (\Phi_L^{-1}(u, t_0))^T du \right] \Phi_L^T(t, t_0) \quad (35)$$

Differentiating (35) shows that $\Sigma_L(t)$ satisfies the Riccati equation

$$\dot{\Sigma}_L(t) = A(t)\Sigma_L(t) + \Sigma_L(t)A^T(t) + B(t)B^T(t) \quad (36)$$

For the time-invariant case, $A_L(t) = A_L$ and $B_L(t) = B_L$, equations (33)-(35) simplify to

$$\begin{aligned}
X_L(t) &= e^{A_L(t-t_0)}X_L(t_0) + \int_{t_0}^t e^{A_L(t-u)}B_L dW_L(u) \\
E[X_L(t)] &= e^{A_L(t-t_0)}E[X_L(t_0)] \\
\Sigma_L(t) &= e^{A_L(t-t_0)}\text{Var}[X_L(t_0)]e^{A_L^T(t-t_0)} + \int_{t_0}^t e^{A_L(t-u)}B_LB_L^Te^{A_L^T(t-u)}du
\end{aligned} \tag{37}$$

It can be seen in (34) and (35) that the mean and variance of the inphase and quadrature components are functions of time. Note that the statistics of the inphase and quadrature components, and therefore the statistics of the STF channel, are time varying. Therefore, these stochastic state space models reflect the TV characteristics of the STF channel. Following the same procedure in developing the STF channel models, the stochastic TV ad hoc channel models are developed in the next section.

5. Stochastic Ad Hoc Channel Modeling

5.1 The Deterministic DPSD of Ad Hoc Channels

Dependent on mobile speed, wavelength, and angle of incidence, the Doppler frequency shifts on the multipath rays give rise to a DPSD. The cellular DPSD for a received fading carrier of frequency f_c is given in (20) and can be described by [25]

$$\frac{S(f)}{pG/\pi f_1} = \begin{cases} \frac{1}{\sqrt{1 - \left(\frac{f-f_c}{f_1}\right)^2}} & , |f-f_c| < f_1 \\ 0 & , \text{otherwise} \end{cases} \tag{38}$$

where f_1 is the maximum Doppler frequency of the mobile, p is the average power received by an isotropic antenna, and G is the gain of the receiving antenna. For a mobile-to-mobile (or ad hoc) link, with f_1 and f_2 as the sender and receiver's maximum Doppler frequencies, respectively, the degree of double mobility, denoted by α is defined by $\alpha = [\min(f_1, f_2) / \max(f_1, f_2)]$, so $0 \leq \alpha \leq 1$, where $\alpha=1$ corresponds to a full double mobility and $\alpha=0$ to a single mobility like cellular link, implying that cellular channels are a special case of mobile-to-mobile channels. The corresponding deterministic mobile-to-mobile DPSD is given by [39-41]

$$\frac{S(f)}{(pG)^2/\pi^2 f_m \sqrt{\alpha}} = \begin{cases} K \left(\frac{1+\alpha}{2\sqrt{\alpha}} \sqrt{1 - \left(\frac{f-f_c}{(1+\alpha)f_m}\right)^2} \right) & , |f-f_c| < (1+\alpha)f_m \\ 0 & , \text{otherwise} \end{cases} \tag{39}$$

where $K(\cdot)$ is the complete elliptic integral of the first kind, and $f_m = \max(f_1, f_2)$. Figure 10 shows the deterministic mobile-to-mobile DPSDs for different values of α 's. Thus, a generalized DPSD has been found where the U-shaped spectrum of cellular channels is a special case.

Here, we follow the same procedure in deriving the stochastic STF channel models in Section 4. The deterministic ad hoc DPSD is first factorized into an approximate n th order even transfer function, and then use a stochastic realization [32] to obtain a state space representation for inphase and quadrature components. The complex cepstrum algorithm [36] is used to approximate the ad hoc DPSD and is discussed next.

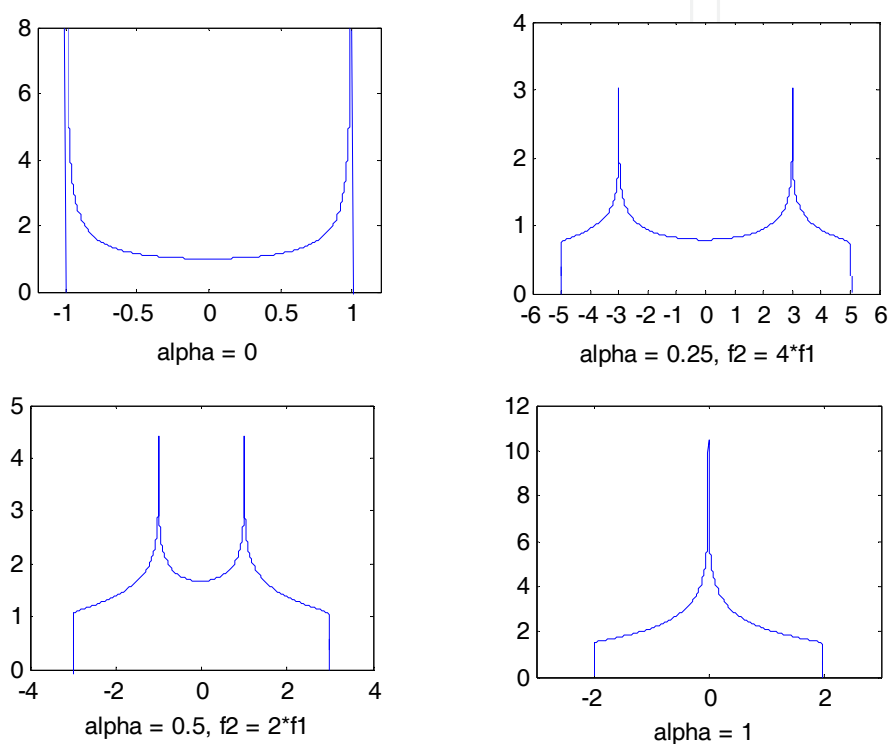


Fig. 10. Ad hoc deterministic DPSDs for different values of α 's, with parameters $f_c = 0$, $f_1 = 1$, and $pG = \pi$.

5.2 Approximating the Deterministic Ad Hoc DPSD

Since the ad hoc DPSD is more complicated than the cellular one, we propose to use a more complex and accurate approximation method: The complex cepstrum algorithm [36]. It uses several measured points of the DPSD instead of just three points as in the simple method (described in Section 4.2). It can be explained briefly as follows: On a log-log scale, the magnitude data is interpolated linearly, with a very fine discretization. Then, using the complex cepstrum algorithm [36], the phase, associated with a stable, minimum phase, real, rational transfer function with the same magnitude as the magnitude data is generated.

With the new phase data and the input magnitude data, a real rational transfer function can be found by using the Gauss-Newton method for iterative search [35], which is used to

generate a stable, minimum phase, real rational transfer function, denoted by $\tilde{H}(s)$, to identify the best model from the data of $H(f)$ as

$$\min_{a,b} \sum_{k=1}^l wt(f_k) |H(f_k) - \tilde{H}(f_k)|^2 \quad (40)$$

where

$$\tilde{H}(s) = \frac{b_{m-1}s^{m-1} + \dots + b_1s + b_0}{s^m + a_{m-1}s^{m-1} + \dots + a_1s + a_0} \quad (41)$$

$b = \{b_{m-1}, \dots, b_0\}$, $a = \{a_{m-1}, \dots, a_0\}$, $wt(f)$ is the weight function, and l is the number of frequency points. Several variants have been suggested in the literature, where the weighting function gives less attention to high frequencies [35]. This algorithm is based on Levi [42]. Figure 11 shows the DPSD, $S(f)$, and its approximation $\tilde{S}(f)$ via different orders using complex cepstrum algorithm. The higher the order of $\tilde{S}(f)$ the better the approximation obtained. It can be seen that approximation with a 4th order transfer function gives a very good approximation.

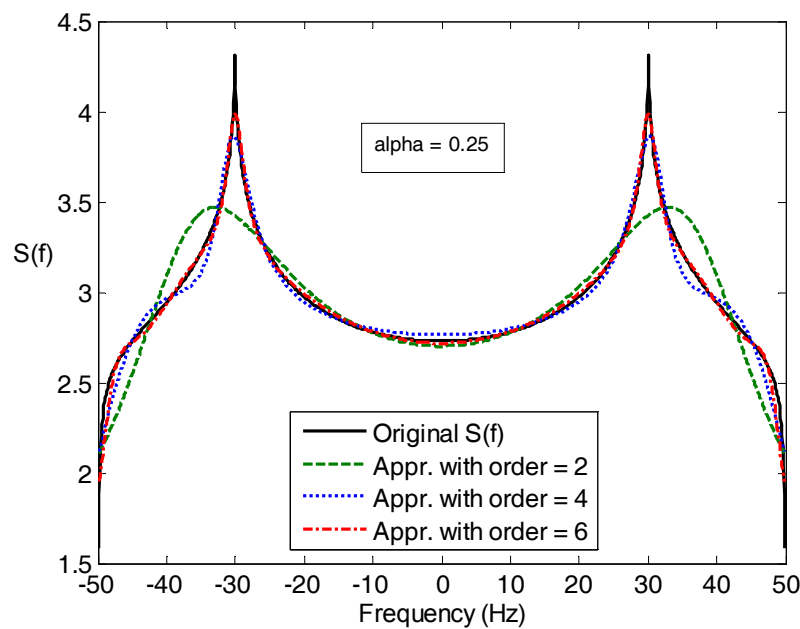
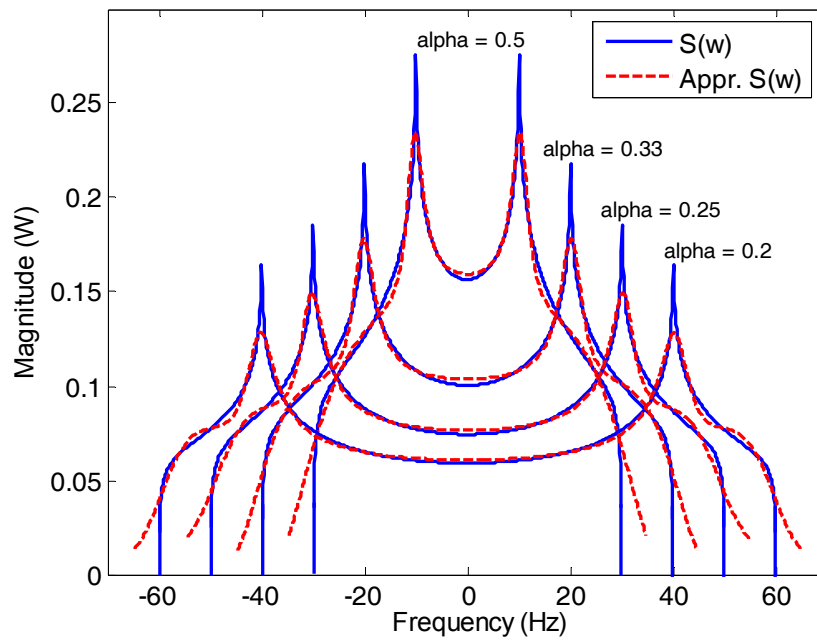


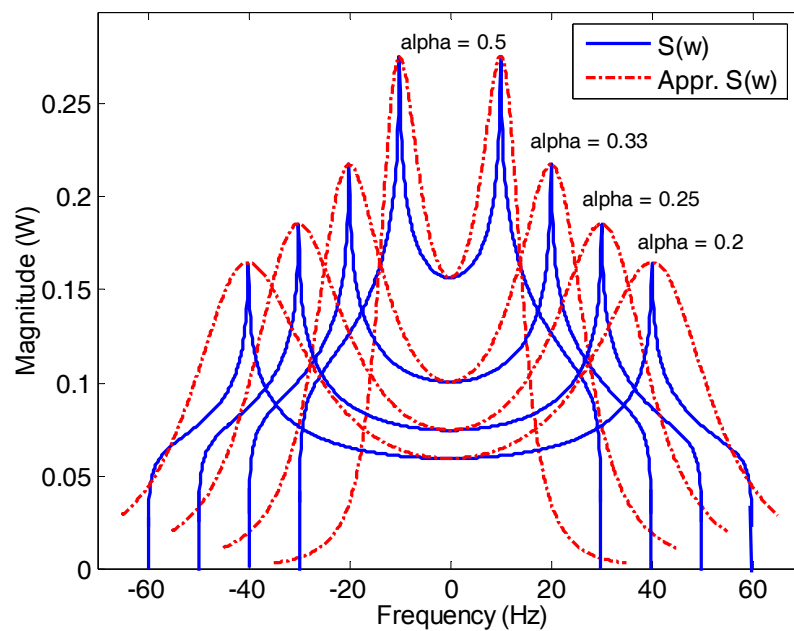
Fig. 11. DPSD, $S(f)$, and its approximations, $\tilde{S}(f)$, using complex cepstrum algorithm for different orders of $\tilde{S}(f)$.

Figure 12(a) and 12(b) show the DPSD, $S(f)$, and its approximation $\tilde{S}(f)$ using the complex cepstrum and simple approximation methods, respectively, for different values of α 's via 4th order even function. It can be noticed that the former gives better approximation

than the latter; since it employs all measured points of the DPSD instead of just three points in the simple method.



(a)



(b)

Fig. 12. DPSD, $S(f)$, and its approximation, $\tilde{S}(f)$, via 4th order function for different α 's using (a) the complex cepstrum, and (b) the simple approximation methods.

5.3 Stochastic Ad Hoc Channel Models

The same procedure as in the STF cellular case is used to develop ad hoc channel models. The stochastic OCF is used to realize (41) for the inphase and quadrature components as [28]

$$\begin{aligned}
 dX_{I,j}(t) &= A_I X_{I,j}(t) dt + B_I dW_j^I(t) \\
 I_j(t) &= C_I X_{I,j}(t) + f_j^I(t) \\
 dX_{Q,j}(t) &= A_Q X_{Q,j}(t) dt + B_Q dW_j^Q(t) \\
 Q_j(t) &= C_Q X_{Q,j}(t) + f_j^Q(t)
 \end{aligned} \tag{42}$$

Where

$$\begin{aligned}
 X_{I,j}(t) &= [X_{I,j}^1(t), X_{I,j}^2(t), \dots, X_{I,j}^m(t)]^T, \quad X_{Q,j}(t) = [X_{Q,j}^1(t), X_{Q,j}^2(t), \dots, X_{Q,j}^m(t)]^T \\
 A_I = A_Q &= \begin{bmatrix} 0 & 1 & 0 & \dots & 0 \\ 0 & 0 & 1 & \dots & 0 \\ \vdots & \vdots & \vdots & \ddots & \vdots \\ 0 & 0 & 0 & \dots & 1 \\ -a_0 & -a_1 & -a_2 & \dots & -a_{m-1} \end{bmatrix}, \quad B_I = B_Q = \begin{bmatrix} b_{m-1} \\ \vdots \\ \vdots \\ b_1 \\ b_0 \end{bmatrix}, \quad C_I = C_Q = [1 \ 0 \ \dots \ 0]
 \end{aligned} \tag{43}$$

$X_{I,j}(t)$ and $X_{Q,j}(t)$ are state vectors of the inphase and quadrature components. $I_j(t)$ and $Q_j(t)$ correspond to the inphase and quadrature components, respectively, $\{W_j^I(t)\}_{t \geq 0}$ and $\{W_j^Q(t)\}_{t \geq 0}$ are independent standard Brownian motions, which correspond to the inphase and quadrature components of the j th path respectively, the parameters $\{a_{m-1}, \dots, a_0, b_{m-1}, \dots, b_0\}$ are obtained from the approximation of the ad hoc DPSD, and $f_j^I(t)$ and $f_j^Q(t)$ are arbitrary functions representing the LOS of the inphase and quadrature components respectively. Equation (42) for the inphase and quadrature components of the j th path can be described as in (28), and the solution of the ad hoc state space model in (42) is similar to the one for STF model described in Section 4.4. The mean and variance of the ad hoc inphase and quadrature components have the same form as the ones for the STF case in (34) and (35), which show that the statistics are functions of time. The general TV state space representation for the ad hoc channel model is similar to the STF state space representation in (31) and (32).

Example 4: Consider a mobile-to-mobile (ad hoc) channel with parameters $v_1 = 36 \text{ km/hr}$ (10 m/s) and $v_2 = 24 \text{ km/hr}$ (6.6 m/s), in which $\alpha = 0.66$. Figure 13 shows time domain simulation of the inphase and quadrature components, and the attenuation coefficient. The inphase and quadrature components have been produced using (42) and (43), while the received signal is reproduced using (30). In Figure 13 Gauss-Newton method is used to approximate the deterministic DPSD with 4th order transfer function.

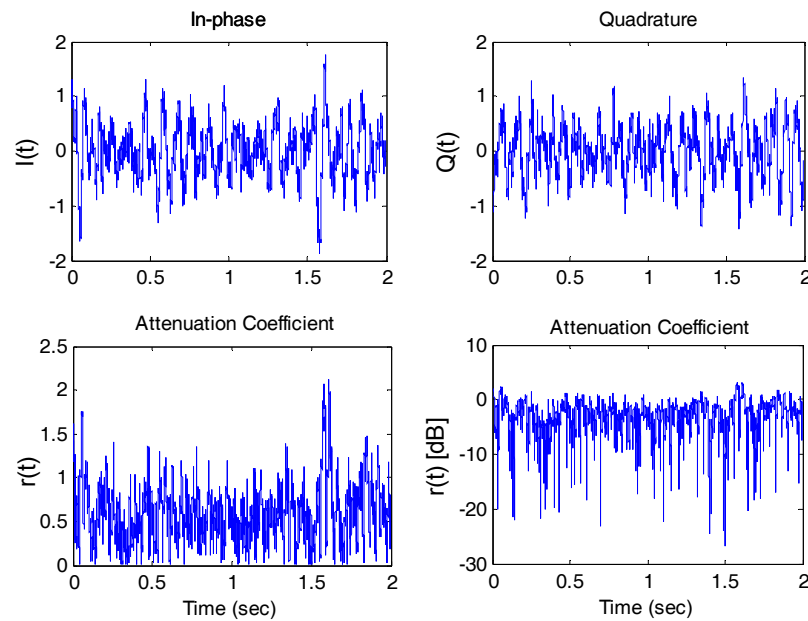


Fig. 13. Inphase and quadrature components $\{I(t), Q(t)\}$, and the attenuation coefficient $r_n(t) = \sqrt{I_n^2(t) + Q_n^2(t)}$, for a mobile-to-mobile channel with $\alpha = 0.66$ in Example 4.

6. Link Performance for Cellular and Ad Hoc Channels

Now, we want to compare the performance of the stochastic mobile-to-mobile link in (42) with the cellular link. We consider BPSK is the modulation technique and the carrier frequency is $f_c = 900\text{MHz}$. We test 10000 frames of $P = 100$ bits each. We assume mobile nodes are vehicles, with the constraint that the average speed over the mobile nodes is 30 km/hr. This implies $v_1 + v_2 = 60\text{km/hr}$, thus for a mobile-to-mobile link with $a = 0$ we get $v_1 = 60\text{km/hr}$ and $v_2 = 0$. The cellular case is defined as the scenario where a link connects a mobile node with speed 30 km/hr to a permanently stationary node, which is the base station. Thus, there is only one mobile node, and the constraint is satisfied. We consider the NLOS case ($f_i = f_Q = 0$), which represents an environment with large obstructions.

The state space models developed in (27) and (42) are used for simulating the inphase and quadrature components for the cellular and ad hoc channels, respectively. The complex cepstrum approximation method is used to approximate the ad hoc DPSD with a 4th order stable, minimum phase, real, and rational transfer function. The received signal is reproduced using (30). Figure 14 shows the attenuation coefficient, $r(t) = \sqrt{I^2(t) + Q^2(t)}$, for both the cellular case and the worst-case mobile-to-mobile case ($\alpha = 1$). It can be observed that a mobile-to-mobile link suffers from faster fading by noting the higher frequency components in the worst-case mobile-to-mobile link. Also it can be noticed that deep fading (envelope less than -12 dB) on the mobile-to-mobile link occurs more frequently and less bursty (48 % of the time for the mobile-to-mobile link and 32 % for the cellular link). Therefore, the increased Doppler spread due to double mobility tends to smear the errors out, causing higher frame error rates.

Consider the data rate given by $R_b = P / T_c = 5$ Kbps which is chosen such that the coherence time T_c equals the time it takes to send exactly one frame of length P bits, a condition where variation in Doppler spread greatly impacts the frame error rate (FER). Figure 15 shows the link performance for 10000 frames of 100 bits each. It is clear that the mobile-to-mobile link is worse than the cellular link, but the performance gap decreases as $\alpha \rightarrow 1$. This agrees with the main conclusion of [40], that an increase in degree of double mobility mitigates fading by lowering the Doppler spread. The gain in performance is nonlinear with α , as the majority of gain is from $\alpha = 0$ to $\alpha = 0.5$. Intuitively, it makes sense that link performance improves as the degree of double mobility increases, since mobility in the network becomes distributed uniformly over the nodes in a kind of equilibrium.

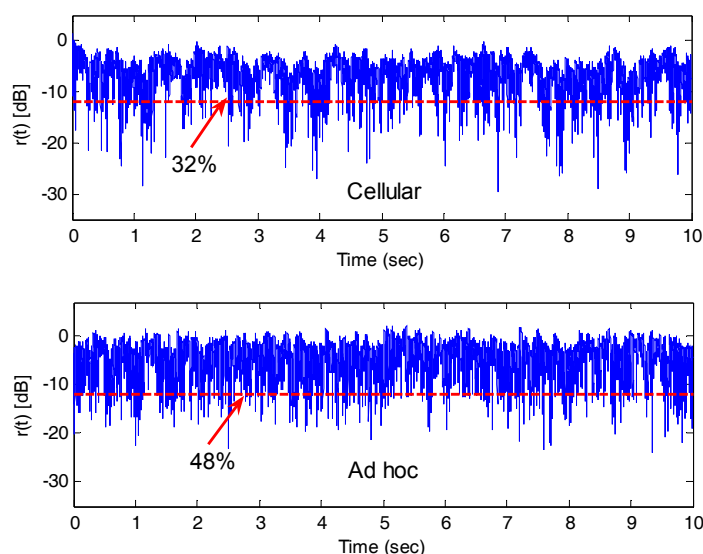


Fig. 14. Rayleigh attenuation coefficient for cellular link and worst-case ad hoc link.

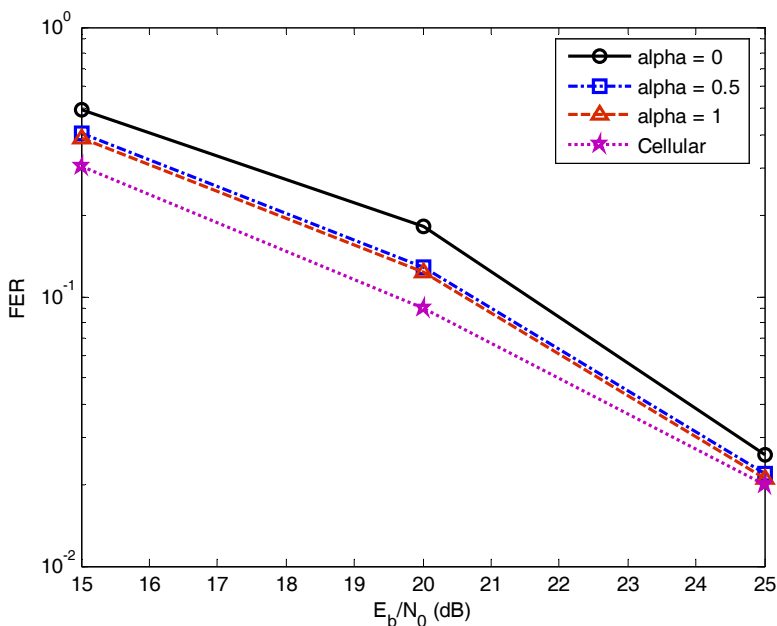


Fig. 15. FER results for Rayleigh mobile-to-mobile link for different α 's and compared with cellular link.

7. Conclusion

In this chapter, stochastic models based on SDEs for LTF, STF, and ad hoc wireless channels are derived. These models are useful in capturing nodes mobility and environmental changes in mobile wireless networks. The SDE models described allow viewing the wireless channel as a dynamical system, which shows how the channel evolves in time and space. These models take into consideration the statistical and time variations in wireless communication environments. The dynamics are captured by a stochastic state space model, whose parameters are determined by approximating the deterministic DPSD. Inphase and quadrature components of the channel and their statistics are derived from the proposed models. The state space models have been used to verify the effect of fading on a transmitted signal in wireless fading networks. In addition, since these models are represented in state space form, they allow well-developed tools of estimation and identification to be applied to this class of problems. The advantage of using SDE methods is due to computational simplicity because estimation and identification algorithms can be performed recursively and in real time.

8. Acknowledgments

This chapter has been co-authored by employees of UT-Battelle, LLC, under contract DE-AC05-00OR22725 with the U.S. Department of Energy. The United States Government retains and the publisher, by accepting the article for publication, acknowledges that the United States Government retains a non-exclusive, paid-up, irrevocable, world-wide license to publish or reproduce the published form of this manuscript, or allow others to do so, for United States Government purposes.

9. References

- [1] F. Molisch, *Wireless communications*. New York: IEEE Press/ Wiley, 2005.
- [2] J. Proakis, *Digital communications*, McGraw Hill, 4th Edition, 2000.
- [3] G. Stüber, *Principles of mobile communication*, Kluwer, 2nd Edition, 2001.
- [4] T.S. Rappaport, *Wireless communications: Principles and practice*, Prentice Hall, 2nd Edition, 2002.
- [5] J.F. Ossanna, "A model for mobile radio fading due to building reflections, theoretical and experimental waveform power spectra," *Bell Systems Technical Journal*, 43, 2935-2971, 1964.
- [6] F. Graziosi, M. Pratesi, M. Ruggieri, and F. Santucci, "A multicell model of handover initiation in mobile cellular networks," *IEEE Transactions on Vehicular Technology*, vol. 48, no. 3, pp. 802-814, 1999.
- [7] F. Graziosi and F. Santucci, "A general correlation model for shadow fading in mobile systems," *IEEE Communication Letters*, vol. 6, no. 3, pp. 102-104, 2002.
- [8] M. Taaghoul and R. Tafazolli, "Correlation model for shadow fading in land-mobile satellite systems," *Electronics Letters*, vol. 33, no. 15, pp.1287-1288, 1997.
- [9] R.H. Clarke, "A statistical theory of mobile radio reception," *Bell Systems Technical Journal*, 47, 957-1000, 1968.

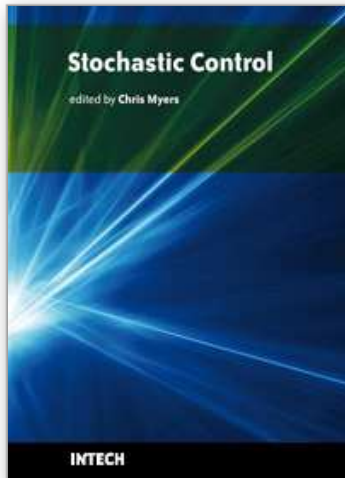
- [10] J.I. Smith, "A computer generated multipath fading simulation for mobile radio," *IEEE Trans. on Vehicular Technology*, vol. 24, no. 3, pp. 39-40, Aug. 1975.
- [11] T. Aulin, "A modified model for fading signal at a mobile radio channel," *IEEE Trans. on Vehicular Technology*, vol. 28, no. 3, pp. 182-203, 1979.
- [12] A. Saleh and R. Valenzuela, "A statistical model for indoor multipath propagation," *IEEE Journal on Selected Areas in Communication*, vol. 5, no. 2, pp. 128-137, Feb. 1987.
- [13] M. Gans, "A power-spectral theory of propagation in the mobile radio environment," *IEEE Trans. on Vehicular Technology*, vol. 21, no. 1, pp. 27-38, 1972.
- [14] A. Duel-Hallen, S. Hu and H. Hallen, "Long-range prediction of fading signals," *IEEE Signal Processing Magazine*, pp. 62-75, May 2000.
- [15] K. Baddour and N.C. Beaulieu, "Autoregressive modeling for fading channel simulation," *IEEE Trans. On Wireless Communication*, vol. 4, No. 4, July 2005, pp. 1650-1662.
- [16] H.S. Wang and Pao-Chi Chang, "On verifying the first-order Markovian assumption for a Rayleigh fading channel model," *IEEE Transactions on Vehicular Technology*, vol. 45, No. 2, pp. 353-357, May 1996.
- [17] C.C. Tan and N.C. Beaulieu, "On first-order Markov modeling for the Rayleigh fading channel," *IEEE Transactions on Communications*, vol. 48, No. 12, pp. December 2000.
- [18] H.S. Wang and N. Moayeri, "Finite-state Markov channel: A useful model for radio communication channels," *IEEE Transactions on Vehicular Technology*, Vol. 44, No. 1, pp. 163-171, February 1995.
- [19] I. Chlamtac, M. Conti, and J.J. Liu, "Mobile ad hoc networking: imperatives and challenges," *Ad Hoc Networks*, vol.1, no. 1, 2003.
- [20] A.S. Akki and F. Haber, "A statistical model for mobile-to-mobile land communication channel," *IEEE Trans. on Vehicular Technology*, vol. 35, no. 1, pp. 2-7, Feb. 1986.
- [21] A.S. Akki, "Statistical properties of mobile-to-mobile land communication channels," *IEEE Trans. on Vehicular Technology*, vol. 43, no. 4, pp. 826-831, Nov. 1994.
- [22] J. Dricot, P. De Doncker, E. Zimanyi, and F. Grenez, "Impact of the physical layer on the performance of indoor wireless networks," *Proc. Int. Conf. on Software, Telecommunications and Computer Networks (SOFTCOM)*, pp. 872-876, Split (Croatia), Oct. 2003.
- [23] M. Takai, J. Martin, and R. Bagrodia, "Effects of wireless physical layer modeling in mobile ad hoc networks," *Proceedings of the 2nd ACM International Symposium on Mobile Ad Hoc Networking & Computing*, Long Beach, CA, USA, Oct. 2001.
- [24] R. Negi and A. Rajeswaran, "Physical layer effect on MAC performance in ad-hoc wireless networks," *Proc. of Commun., Internet and Info. Tech. (CIIT)*, 2003.
- [25] W. Jakes, *Microwave mobile communications*, IEEE Inc., NY, 1974.
- [26] B. Sklar, *Digital communications: Fundamentals and applications*. Prentice Hall, 2nd Edition, 2001.
- [27] C.D. Charalambous and N. Menemenlis, "Stochastic models for long-term multipath fading channels," *Proc. 38th IEEE Conf. Decision Control*, pp. 4947-4952, Phoenix, AZ, Dec. 1999.
- [28] M.M. Olama, S.M. Djouadi, and C.D. Charalambous, "Stochastic differential equations for modeling, estimation and identification of mobile-to-mobile communication channels," *IEEE Transactions on Wireless Communications*, vol. 8, no. 4, pp. 1754-1763, 2009.

- [29] M.M. Olama, K.K. Jaladhi, S.M. Djouadi, and C.D. Charalambous, "Recursive estimation and identification of time-varying long-term fading channels," *Research Letters in Signal Processing*, Volume 2007 (2007), Article ID 17206, 5 pages, 2007.
- [30] M.M. Olama, S.M. Djouadi, and C.D. Charalambous, "Stochastic power control for time varying long-term fading wireless networks," *EURASIP Journal on Applied Signal Processing*, vol. 2006, Article ID 89864, 13 pages, 2006.
- [31] C.D. Charalambous and N. Menemenlis, "General non-stationary models for short-term and long-term fading channels," *EUROCOMM 2000*, pp. 142-149, April 2000.
- [32] B. Oksendal, *Stochastic differential equations: An introduction with applications*, Springer, Berlin, Germany, 1998.
- [33] W.J. Rugh, *Linear system theory*, Prentice-Hall, 2nd Edition, 1996.
- [34] R.E.A.C. Paley and N. Wiener, "Fourier transforms in the complex domain," *Amer. Math. Soc. Coll., Am. Math.*, vol. 9, 1934.
- [35] J.E. Dennis Jr., and R.B. Schnabel, *Numerical methods for unconstrained optimization and nonlinear equations*, NJ: Prentice-Hall, 1983.
- [36] A.V. Oppenheim and R.W. Schaffer, *Digital signal processing*, Prentice Hall, New Jersey, 1975, pp. 513.
- [37] <http://www.mathworks.com/>
- [38] P.E. Caines, *Linear stochastic systems*, New-York Wiley, 1988.
- [39] R. Wang and D. Cox, "Channel modeling for ad hoc mobile wireless networks," *Proc. IEEE VTC*, 2002.
- [40] R. Wang and D. Cox, "Double mobility mitigates fading in ad hoc wireless networks," *Proc. of the International Symposium on Antennas and Propagation*, vol. 2, pp. 306-309, 2002.
- [41] C.S. Patel, G.L. Stuber, and T.G. Pratt, "Simulation of Rayleigh-faded mobile-to-mobile communication channels," *IEEE Trans. on Comm.*, vol. 53, no. 11, pp. 1876-1884, 2005.
- [42] E.C. Levi, "Complex curve fitting," *IRE Trans. on Automatic Control*, vol. AC-4, pp. 37-44, 1959.

IntechOpen

IntechOpen

IntechOpen



Stochastic Control

Edited by Chris Myers

ISBN 978-953-307-121-3

Hard cover, 650 pages

Publisher Sciyo

Published online 17, August, 2010

Published in print edition August, 2010

Uncertainty presents significant challenges in the reasoning about and controlling of complex dynamical systems. To address this challenge, numerous researchers are developing improved methods for stochastic analysis. This book presents a diverse collection of some of the latest research in this important area. In particular, this book gives an overview of some of the theoretical methods and tools for stochastic analysis, and it presents the applications of these methods to problems in systems theory, science, and economics.

How to reference

In order to correctly reference this scholarly work, feel free to copy and paste the following:

Mohammed Olama, Seddik Djouadi and Charalambos Charalambous (2010). Wireless Fading Channel Models: from Classical to Stochastic Differential Equations, Stochastic Control, Chris Myers (Ed.), ISBN: 978-953-307-121-3, InTech, Available from: <http://www.intechopen.com/books/stochastic-control/wireless-fading-channel-models-from-classical-to-stochastic-differential-equations>

INTECH
open science | open minds

InTech Europe

University Campus STeP Ri
Slavka Krautzeka 83/A
51000 Rijeka, Croatia
Phone: +385 (51) 770 447
Fax: +385 (51) 686 166
www.intechopen.com

InTech China

Unit 405, Office Block, Hotel Equatorial Shanghai
No.65, Yan An Road (West), Shanghai, 200040, China
中国上海市延安西路65号上海国际贵都大饭店办公楼405单元
Phone: +86-21-62489820
Fax: +86-21-62489821

© 2010 The Author(s). Licensee IntechOpen. This chapter is distributed under the terms of the [Creative Commons Attribution-NonCommercial-ShareAlike-3.0 License](#), which permits use, distribution and reproduction for non-commercial purposes, provided the original is properly cited and derivative works building on this content are distributed under the same license.

IntechOpen

IntechOpen